- Technical Paper -

TIME-DEPENDENT RELIABILITY ASSESSMENT OF SHIELD TUNNELS UNDER CHLORIDE AND HYDRAULIC PRESSURE HAZARDS

Zhengshu HE[*1] and Mitsuyoshi AKIYAMA[*2]

ABSTRACT

In contrast to ground reinforced concrete structure systems, shield tunnels in coastal regions undergo more complicated and rapid deteriorating processes owing to the coupling effects of multiple mechanical and environmental stressors during the tunnel life-cycle. In this paper, a time-dependent structural reliability assessment method considering the hazards associated with chloride around the shield tunnel and the impact of hydrostatic pressure is proposed. Monte Carlo Simulation is used in conjunction with a failure probability estimation associated with the occurrence of concrete cracking due to the steel corrosion.

Keywords: shield tunnel, life-cycle reliability, hazard assessment, chloride attack, hydrostatic pressure

1. INTRODUCTION

For cities located in coastlands or regions with numerous lakes and rivers, shield tunnels have gradually become a main way to cross waters in the water-rich stratums. However, reinforced concrete (RC) tunnel linings are exposed to chemical attacks from highly concentrated aggressive agents. Aggressive agents, such as chlorides and sulfates, diffuse under concentration gradients and/or permeate with liquids due to the high hydrostatic pressure in the linings [1, 2]. This process often leads to premature steel corrosion and concrete cracking. Therefore, shield tunnels require higher structural performance and durability in aggressive environments; in order to accurately evaluate the structural performance of a shield tunnel during its life-cycle, the coupling effects of aggressive agents and high hydrostatic pressure on the deterioration of the shield tunnels need to be taken into consideration.

Kudo and Guo [3] studied the durability and anti-corrosion properties of the highway shield tunnel crossing Tokyo Bay with a durability test. Sun [4] proposed a methodology and corresponding testing methods for the durability design of a subsea tunnel in China. Over the past few decades, researches [5-7] have mainly focused on the qualitative durability assessment and lifetime prediction of underwater tunnels based on corrosion testing of the RC components and on-site monitoring. Recently, although probabilistic methods for the deterioration evaluation of underwater tunnels [8, 9] have been gradually reported, there has been a lack of research on marine environmental hazard assessments and time-dependent reliability analyses.

In this paper, considering that the deterioration of shield tunnels depends on structural locations and their surroundings, the hazards associated with chloride around tunnels in a coastal region are investigated. The chloride transportation in the segmental linings is examined with emphasis on the impact of hydrostatic pressure. Two transport approaches of chloride ions including the diffusion process and the advection process are suggested, and thus the time to corrosion initiation is estimated. Finally, a time-dependent structural reliability analysis of shield tunnels in a marine environment is accomplished using the Monte Carlo Simulation (MCS).

2. HAZARD ASSESSMENT ASSOCIATED WITH MARINE CHLORIDES

2.1 Attenuation Law of Underground Chlorides in Coastal Regions

Regional environments influence the deterioration processes of RC structures, and different environmental conditions will cause RC structures to undergo different deterioration processes. As a result, environmental conditions should be quantitatively assessed and applied to evaluate the environmental hazards for tunnel structures in different regions. With respect to tunnels located in different coastal regions, it is assumed that the attenuation of underground chloride ions around tunnels, C_{soil} (ppm, i.e., 1 mg/L), only depends on the chloride concentration of coastal waters, C_{sea} (ppm), and the distance d (km) from the coastline to the structures.

Observed values on Xiamen [10] are used herein to obtain the attenuation relationship between the chloride content in the underground, C_{soil}, and the distance from the coastline. There are 18 sites on Xiamen Island for collecting data on C_{soil}, and a regression analysis using least squares method to reflect non-linear attenuation trend of coastal hazards associated with chloride was conducted based on [11], as shown in Fig. 1. Considering the influence of chloride content in the coastal waters, C_{sea}, the attenuation of C_{soil} in horizontal direction is provided as follows:

$$C_{soil} = 0.62 \cdot C_{sea} \cdot 0.63^{d} \quad (1)$$

*1 Graduate School of Creative Sciences and Engineering, Waseda University, JCI Student Member
*2 Professor, Dept. of Civil and Environmental Engineering, Waseda University, JCI Member

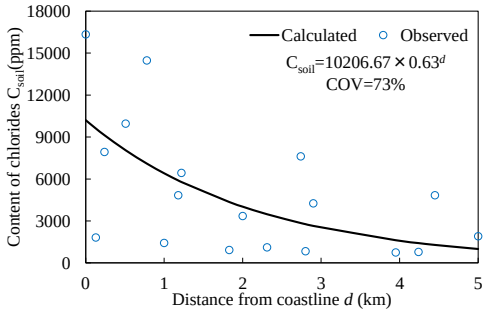

Fig. 1 Content of underground chlorides versus distance from coastline in Xiamen

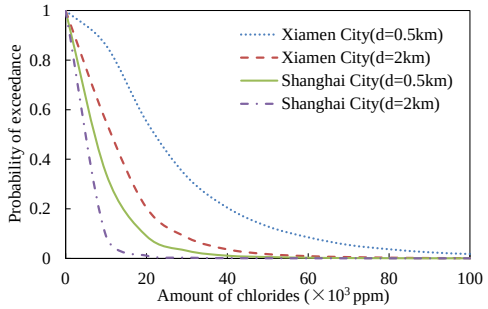

Fig. 2 Hazard curves for content of underground chlorides at two coastal cities with the distance of 0.5 km and 2 km from coastline

Underground environments around shield tunnel are complex, non-continuous and uncertain. Since the data of underground chlorides at different coastal regions is very limited, it is difficult to consider the influence of geological formations, geotechnical properties around structure, dilution of fresh water on surface, precipitation, tunnel depth and the difference in coastal topography on the content of underground chlorides collected at each location. To consider the uncertainties involved in the prediction of underground chlorides around tunnels, a parameter associated with model error should be included in the attenuation equations.

2.2 Hazard Associated with Chlorides around the Tunnel

Considering model uncertainty, the attenuation, Eq. 2, can be expressed as follows:

$$C_{Soil} = X_R \cdot \left[0.62 \cdot \left(X_S \cdot C_{Sea}\right) \cdot 0.63^d\right] \tag{2}$$

where X_R is the lognormal random variable related to estimation of chloride content in soil; and X_S is the normal random variable associated with the marine chloride content at different coastal regions.

The probability that C_{soil} at a specific site exceeds an assigned value c_{soil} is described as follows:

$$q(c_{Soil}) = P(C_{Soil} > c_{Soil}) = \int_0^\infty P(X_R > \frac{c_{Soil}}{0.62 \cdot X_S C_{Sea} \cdot 0.63^d}) \times f(X_S) dX_S \tag{3}$$

where $f(X_S)$ is the probability density function of X_S.

Hazard curves for tunnel structures in different cities using Eq. 3 are shown in Fig. 2.

3. FAILURE PROBABILITY ESTIMATION ASSOCIATED WITH THE CORROSION CRACKS

3.1 Chloride Transport in Segmental Linings under Hydrostatic Pressure

For a few decades, most researchers [4, 9] have estimated the life-cycle performance of undersea tunnels only considering the diffusion of chloride ions in RC linings, and Fick's diffusion law was adopted to predict the lifetime of undersea tunnels. However, due to the effect of high hydrostatic pressure on the tunnels, structures withstand a large water pressure gradient between the inside and outside walls, and the chloride motion in the linings is associated with external water pressure as proved by experimental results [1, 2]. As a result, considering the action of hydrostatic pressure and the water environment, it is thought that the coupling effects of diffusion and advection drive the chloride motion. In detail, diffusion results in the transport of chloride ions from the part of high ion concentration to that of lower ion concentration. Meanwhile, advection means ions transport due to the bulk motion of the carrier fluid, including matric potential (i.e., capillary) and pressure potential (i.e., permeation).

Chloride transport in concrete is assumed to be under steady-state conditions, thus diffusion flux of the free chloride ions using Fick's 1st diffusion law is usually applied and expressed as follows:

$$J_d = -D\nabla C_f \tag{4}$$

where J_d is the diffusion flux of free chloride ions, kg/(m^2·s); D is the chloride diffusion coefficient of concrete, m^2/s; ∇ is the nabla operator; and C_f is the volume concentration of free chloride dissolved in the pore solution, kg/m^3. In particular, the negative sign in Eq. 4 indicates that diffusion occurs with the concentration reduction.

The advection flux can be expressed as follows:

$$J_a = C_f u \tag{5}$$

where J_a is the advection flux of free chloride ions, kg/(m^2·s); and u is the average velocity of chloride, m/s.

Therefore, the total flux of free chloride ions is described as follows:

$$J_{cl} = J_d + J_a \tag{6}$$

where J_{cl} is the total flux of free chloride ions, kg/(m^2·s).

Based on the mass conservation law of chloride ions, the governing differential equation of chloride movement is provided by:

$$\frac{\partial C_f}{\partial t} + \nabla J_{cl} = \frac{\partial C_f}{\partial t} + \nabla(uC_f - D\nabla C_f) = 0 \tag{7}$$

$$\frac{\partial C_f}{\partial t} = D\frac{\partial^2 C_f}{\partial x^2} - u\frac{\partial C_f}{\partial x} \tag{8}$$

With respect to Eq. 8, Ogata and Banks [12] presented an analytic solution for saturated concrete, which is described as follows:

$$C(c,t) = \frac{C_s}{2}\left[erf\left(\frac{c-ut}{\sqrt{4Dt}}\right) + e^{\frac{uc}{D}} erfc\left(\frac{c+ut}{\sqrt{4Dt}}\right)\right] \tag{9}$$

where for shield tunnel structures, x is the depth from the outside wall of linings, mm; t is the time after structural construction, year; C_s is the chloride content at the surface, kg/m^3; u is the average velocity of the

chloride motion, mm/year; D is the chloride ion transportation coefficient in concrete, mm^2/year; *erfc* $(\cdot)$ is the complementary error function, *erfc*$(\cdot) = 1 - erf(\cdot)$; and *erf* $(\cdot)$ is the error function.

A one-dimensional flow seeping through concrete under pressure is regarded as a laminar flow, so the velocity equation of pressurized seeping flow is described based on Darcy's Law as follows [13]:

$$u_w = -K_S \nabla H = -\frac{K_S}{\rho_w g} \nabla P_w \tag{10}$$

where u_w is the flow velocity of liquid, mm/year; K_s is the permeability coefficient, mm/year; H is the hydraulic head, m; ρ_w is the water density, kg/m^3; and P_w is the hydraulic pressure of the flow path, MPa.

According to Eq. 10, Murata et al. [13] proposed two methods to evaluate watertight properties of concrete and the average penetration depth of water under different water pressures with time. For the Darcy seepage flow [13], since the external water pressure P_w is less than 0.15 MPa, the Darcy flow velocity is constant over time and space; the hydraulic gradient becomes linear. The penetration depth of water χ (mm) using Darcy seepage model is provided by:

$$\chi = \sqrt{\frac{2K_s P_w}{\rho_w g} t} \tag{11}$$

Meanwhile, for the seepage diffusive flow [13] that external water pressure P_w is larger than 0.15 MPa, the high water pressure as internal deformation becomes significant, and the flow velocity and hydraulic gradient are variable over time and space. Thus, the penetration depth of water χ (mm) is described using high pressure seepage model as follows:

$$\chi = \sqrt{4\frac{\gamma_0^2 \xi^2}{\alpha} t} \tag{12}$$

where ξ is the coefficient of water pressure, mm^2/year, ξ = 0.4104 ln(P_w) + 0.995; α is correction factor for pressurized time (i.e. $\alpha = (365\times24\times60^2\times t)^{3/7}$; γ^2_0 is the initial diffusion coefficient, mm^2/year, $\gamma^2_0 = (K_s K_v) / (\rho_w g)$; K_v is the volumetric modulus of elasticity when considering substances of water and concrete, expressed by $1/K_v = v / K_c + (1-v) / K_w$, K_c is volumetric modulus of elasticity of concrete body, K_w is volumetric modulus of elasticity of water, and v is volumetric ratio of concrete body; and t is pressurized time, year.

Since the size of a chloride ion is much less than the size of a water molecule, the permeation speed of a chloride ion is much slower than that of water in the concrete, and the transport velocity of a chloride ion is approximately 53% that of water [4]. The average flow velocity of a chloride ion under water pressure is provided by:

$$u = 0.53\chi / t \tag{13}$$

In particular, when the external water pressure P_w is very low (i.e., u is close to zero), the advection process of chloride can be ignored. Therefore, Eq. 9 can be simplified as follows, which is the diffusion equation of chloride based on Fick's second law.

$$C(x,t) = C_s\left[1 - erf\left(\frac{x}{\sqrt{4Dt}}\right)\right] \tag{13}$$

3.2 Reinforcement Corrosion Initiation

The degree of contact with chloride environment has a significant effect on the level of the surface chloride content C_s. In terms of the underground environment in coastal regions, the surface chloride C_s of the shield tunnel is assumed to be approximately equal to the chloride content of soil, and it may not change with time due to the chemical equilibrium for the concrete exposed to infinite seawater [14]. Therefore, the surface chloride C_s is described as follows:

$$C_S = X_1 \cdot 0.001 C_{Soil} \tag{14}$$

where C_s is the chloride content on the outside wall surface of tunnel, kg/m^3; C_{Soil} is the chloride content of the soil, ppm; and X_1 is the lognormal random variable representing model uncertainty.

As the total amount of chloride around rebar accumulates and reaches critical threshold of chloride content C_{cr} (kg/m^3), the corrosion of rebar starts. Thus, the time t_1 to corrosion initiation can be obtained using the following event:

$$g_1 = X_2 C_{cr} - C(c,t) < 0 \tag{15}$$

$$C(c,t) = X_3 \frac{C_s}{2}\left[erf\left(\frac{c-ut}{\sqrt{4Dt}}\right) + e^{\frac{uc}{D}} erfc\left(\frac{c+ut}{\sqrt{4Dt}}\right)\right] \tag{16}$$

$$D = 10^{-6.77(W/C)^2 + 10.10(W/C) - 1.14} \tag{17}$$

where C_{cr} is the critical threshold of chloride content, kg/m^3; c is the concrete cover specified in design, mm; t is the time after construction, year; W/C is the ratio of water to cement; D is the chloride ion transportation coefficient in concrete, mm^2/year; u is the average velocity of chloride motion, mm/year. X_2 is the Gaussian variable associated with the evaluation of C_{cr}; and X_3 is the lognormal variable representing the model uncertainty associated with estimation of $C(c, t)$.

In particular, the chloride coefficient of diffusion (Eq. 17) [11] was obtained by the data reported by Maeda et al. [15], which is used for concrete, including ordinary Portland cement (OPC). With respect to the critical threshold of chloride content C_{cr}, the value of C_{cr} exhibits a high discretization because of material property and environment. For the environment with frequently changing humidity or constant humidity between 90% and 95%, the critical content is the lowest; however, for the submerged structures lacking oxygen, the C_{cr} is higher [16]. Based on the previous reports in [16, 17], C_{cr} is assumed in this study to be 2.8 kg/m^3, and X_2 is treated as a Gaussian random variable with a mean and COV equal to 1.0 and 0.375, respectively.

3.3 Corrosion Crack Occurrence

As the passive film is broken by chloride ions, the metallic Fe at the anode is oxidized to form ferrous ions that can react with hydroxyl ions to produce ferrous hydroxide and then can be further converted to hydrated ferric oxide. Since the various iron oxides have volumes 2-6 times that of iron, a large volume

Table 1 RC Corrosion Rate Review in Submerged Environment (μm/year)

	Corrosion rate	Condition	Case	
J.A. Gonzalez et al [18]	11.6~34.8	Active Corrosion	Lab	Specimen
A. Costa et al [19]	<11.6 81.2	Passive Condition Construction Joint	On-site	Bridge (Portugal)
M. T. Walsh et al [20]	5~35	Pilings of undersea	On-site	Bridge
C. Gong et al [21]	1.16~8.12 58~116 11.6~92.8	Initiation Inside wall Outside wall	On-site	Tunnel (Xiangan Subsea Tunnel, China)

Table 2 Parameters of random variables

Variables	Distribution	Mean	COV
Chloride content in soil (X_R)	Lognormal	1.00	0.73
Marine chloride content (X_S)	Normal	1.00	0.043 (Xiamen) 0.155 (Shanghai)
C_s-C_{soil} equation (X_1)	Lognormal	1.43	1.08
Critical threshold chloride content at occurrence of steel corrosion (X_2)	Normal	1.00	0.375
Estimation of chloride transport (X_3)	Lognormal	1.24	0.906
Critical threshold of corrosion amount at crack initiation (X_4)	Lognormal	1.00	0.352
Corrosion rate (X_5)	Lognormal	1.00	0.58

expansion of rust formation causes internal stress and induces cover concrete segment cracks when the total amount of steel corrosion product Q_b exceeds the critical threshold of corrosion associated with crack initiation Q_{cr}. According to Akiyama et al. [11], the probability associated with the corrosion crack occurrence is estimated by the following performance function:

$$g_2 = X_4 Q_{cr}(c) - Q_b(V_1, t_1, t) < 0 \tag{18}$$

where

$$Q_{cr}(c) = \eta(W_{c1} + W_{c2}) \tag{19}$$

$$W_{c1} = \frac{\rho_s}{\pi(\gamma - 1)}\left[\alpha_0\beta_0 \frac{0.22\left\{2(c+\phi)^2 + \phi^2\right\}}{E_c(c+\phi)} f_c^{2/3}\right] \tag{20}$$

$$W_{c2} = \alpha_1\beta_1 \frac{\rho_s}{\pi(\gamma - 1)} \frac{c+\phi}{5c+3\phi} w_c \tag{21}$$

$$Q_b(V_1, t_1, t) = X_5 \rho_s V_1 (t - t_1) \tag{22}$$

ρ_s is the steel density, 7.85 mg/mm^3; γ=3.0 is the expansion rate of the volume of the corrosion product; f_c is the concrete strength, MPa; w_c is set to 0.1 mm as the crack width of first cracking; E_c is the modulus of elasticity of concrete, MPa; ϕ is the diameter of the steel bar, mm; V_1 is the corrosion rate of the steel bar before the occurrence of a corrosion crack, mm/year; α_0, β_0, α_1 and β_1 are the coefficients taking into account the effects of concrete cover, steel bar diameter and concrete strength; η is the correction factor; X_4 is the lognormal random variable representing the model uncertainty associated with the estimation of Q_{cr}; and X_5 is the lognormal random variable related to the corrosion rate.

Based on Eqs. 18 to 22, the time t_2 to corrosion crack occurrence is described as:

$$t_2 = t_1 + \frac{X_4 Q_{cr}(c)}{X_5 \rho_s V_1} \tag{23}$$

Generally, the corrosion rate of tunnels is higher than that of ground structures due to more serious service environments, especially for the tunnels in the coastal regions with high humidity and high chloride content. According to the monitoring corrosion rate (see Table 1) of RC structures in aggressive environments including submerged environments, the computation of the amount of rebar corrosion is made by assuming that the corrosion rate is 7.7 μm/year before the occurrence of corrosion cracking and without loading ($V_{1,\ f=0}$). Meanwhile, X_5 is assumed as a lognormal with a mean and COV equal to 1.0 and 0.58, respectively, based on previous research [11]. Finally, considering the effect of different loading levels on the corrosion rate based on a previous study [22], the corrosion rate of the segment under different load levels can be expressed as $V_{1f} = 7.78\ e^{0.43f}$.

4. ILLUSTRATIVE EXAMPLE

It is widely recognized that time-dependent probability-based concepts and methods provide a more scientific basis for estimating the life-cycle performance of a structural system, and the failure probability of a structural system during its life-cycle can be defined as a probability of violating any of the limit states indicating its failure modes. In this study, first corrosion-induced cracking was regarded as the limit state of structural failure, and the probability that the cracking occurs before the time t_c is defined as follows:

$$P_f(t) = P\left(t_2 \le t_c\right) \tag{24}$$

A Monte Carlo analysis was conducted to obtain the failure probability of shield tunnels with a sample size of 10,000, and two coastal cities of Xiamen and Shanghai were selected to illustrate the influence of coastal chloride hazard in different regions on the failure probability of tunnels. All parameters of the random variable X_i (i=S, R, 1, 2, 3, 4, 5) involved in the calculation of failure probability using MCS are summarized in Table 2. Finally, the time-dependent

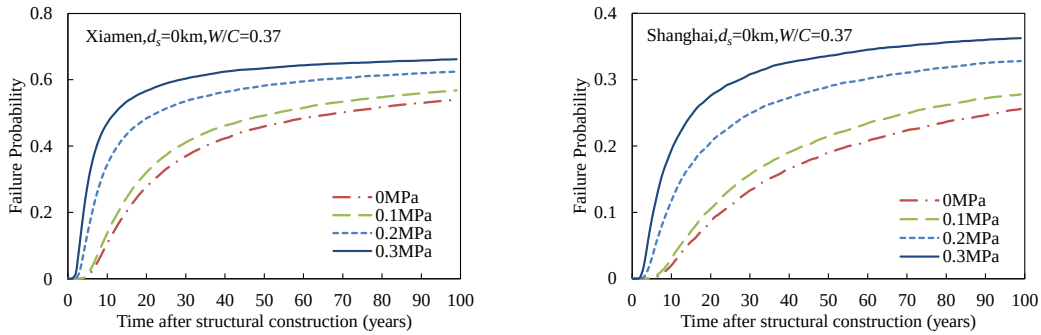

(a) Xiamen City (d_s = 0 km) (b) Shanghai City (d_s = 0 km)

Fig. 3 Failure Probability of Shield Tunnel under Different Hydrostatic Pressure

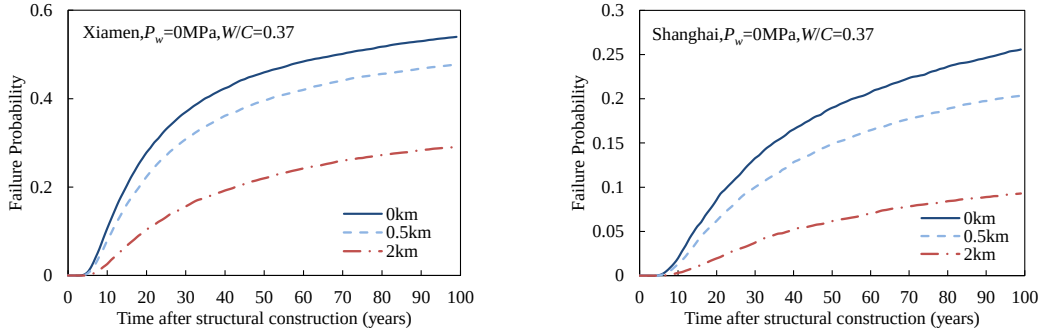

(a) Xiamen City (P_w =0 MPa) (b) Shanghai City (P_w =0 MPa)

Fig. 4 Failure Probability of Shield Tunnel with the Different Distance from Coastline

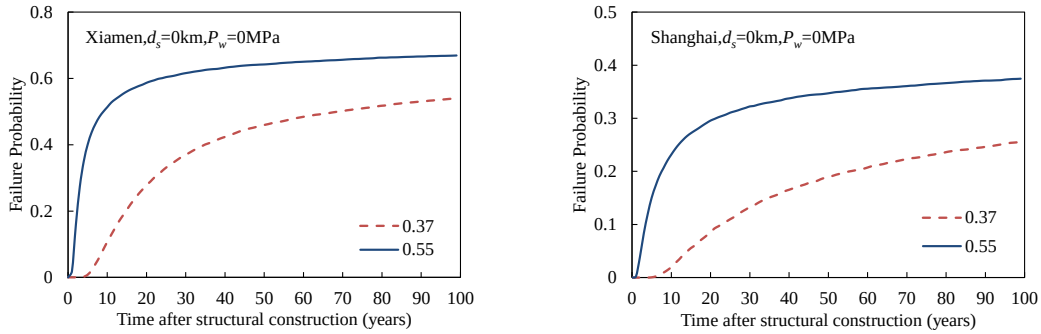

(a) Xiamen City (d_s = 0 km) (b) Shanghai City (d_s = 0 km)

Fig. 5 Failure Probability of Shield Tunnel with Different Ration of Water to Cement

failure probability of the shield tunnel located in Xiamen and Shanghai under different conditions are presented in Figs. 3-5.

Fig. 3 reveals that a greater hydrostatic pressure leads to higher failure probability of shield tunnels. Especially for a shield tunnel under a high hydrostatic pressure condition (i.e., P_w exceeds 0.15 MPa), a significant increase of failure probability of the shield tunnel occurs at a few decades after its construction; 10 years for the tunnels at Xiamen and 30 years for the tunnels at Shanghai.

Meanwhile, the higher chloride content also has a remarkable influence on the failure probability of the shield tunnel. The shield tunnel at Xiamen with higher chloride content undergoes higher failure probability and faster deterioration than that at Shanghai. The reason for this phenomenon is that the transport process of chloride is associated with the hydrostatic pressure and chloride content; higher hydrostatic pressure and/or chloride content allows the chloride ions to permeate more quickly and thus reach the critical threshold of corrosion initiation.

Fig. 4 shows that higher failure probability occurs at the shield tunnel near the marine environment due to the higher chloride hazard, and the probability decreases with the increasing distance from the coastline. Moreover, the failure probability of the shield tunnel subjected to chloride attacks is also significantly influenced by the material property of the segments. As shown in Fig. 5, since the chloride transport process is associated with the ratio of water to cement (i.e., K_s and D), the failure probability of the shield tunnels at Xiamen and Shanghai using the higher ratio of water to cement (i.e. W/C = 0.55) increases by 24% and 47%, respectively, compared with that using the lower ratio of water to cement (i.e. W/C = 0.37). Therefore, the influence of the material property changes on the failure probability is remarkable.

5. CONCLUSIONS

(1) A computational procedure to establish the probabilistic hazard curves of the chloride around the shield tunnel in a coastal region was proposed; this hazard curve can quantify the effect of the aggressive environment on the shield tunnels.

(2) This paper described the probabilistic method for evaluating the chloride transport process in segmental linings with the impact of hydrostatic pressure, and thus the time to corrosion initiation can be estimated considering the combined effect. Under the hydrostatic pressure, chloride ions can permeate more quickly in the segmental linings. This results in the higher failure probability of undersea shield tunnel.

(3) Future work will involve the proposed method in this paper in connection with the damage model, illustrating the corrosion-induced deterioration process of segments [22], in order to account for the life-cycle structural performance of shield tunnels in an aggressive environment.

REFERENCES

[1] Zhang, Y., Li, X., and Yu, G., "Chloride Transport in Undersea Concrete Tunnel," Advances in Materials Science and Engineering, 2016, pp.1-10.

[2] Jin, Z., Zhao, T., Gao, S., and Hou, B., "Chloride ion penetration into concrete under hydraulic pressure," Journal of Central South University, Vol.20, No.12, 2013, pp. 3723-3728.

[3] Kudo, I., and Guo, S., "Study on durability and anti-corrosion: Trans-Tokyo bay highway shield tunnel," Collection of Translations on Tunnelling (Modern Tunnelling Technology), Vol.10, 1994, pp.20-28.

[4] Sun, J., "Durability problems of lining structures for Xiamen Xiang'an subsea tunnel in China," Journal of Rock Mechanics and Geotechnical Engineering, Vol.3, No.4, 2011, pp.289-301.

[5] Lei, M., Peng, L., and Shi, C., "Durability evaluation and life prediction of shield segment under coupling effect of chloride salt environment and load," Journal of Central South University (Science and Technology), Vol.46, No.8, 2015, pp.3092-3099.

[6] Fagerlund, G., "Penetration of chloride through a submerged concrete tunnel," Report TVBM-7077, 1995, pp.1-17.

[7] Funahashi, M., "Corrosion of underwater reinforced concrete tunnel structures," Corrosion, 2013, pp.1-15.

[8] Bagnoli, P. et al., "A method to estimate concrete hydraulic conductivity of underground tunnel to assess lining degradation," Tunnelling and Underground Space Technology, Vol.50, 2015, pp. 415-423.

[9] Song, H., Pack, S., and Ann, K., "Probabilistic assessment to predict the time to corrosion of steel in reinforced concrete tunnel box exposed to sea water," Construction and Building Materials, Vol.23, 2009, pp.3270-3278.

[10] Guo, Z., Huang, Y., Cai, M., and Liu, G., "Nutrition Content and Indicator Value of Chlorion for Groundwater in Xiamen Island," Site Investigation Science and Technology, Vol.3, 2004, pp.47-50.

[11] Akiyama, M., Frangopol, D.M. and Yoshida, I., "Time-dependent reliability analysis of existing RC structures in a marine environment using hazard associated with airborne chlorides," Engineering Structures, Vol.32, 2010, pp.3768-3779.

[12] Ogata, A., and Banks, R.B., "A Solution of the differential equation of longitudinal dispersion in porous media," US Department of Interior, Washington, DC, USA, 1961.

[13] Murata, J., Ogihara, Y., Koshikawa, S., and Itoh, Y., "Study on watertightness of concrete," ACI Materials Journal, No.101, 2004, pp.107-116.

[14] Ann, K.Y., Ahn, J.H., and Ryou, J.S., "The importance of chloride content at the concrete surface in assessing the time to corrosion of steel in concrete structures," Construction and Building Materials, Vol.23, 2009, pp.239-245.

[15] Maeda, S., Takewaka, K., and Yamaguchi, T., "Quantification of chloride diffusion process into concrete under marine environment by analysis of salt damage data base," Journal of Materials, Concrete Structures and Pavements, JSCE, Vol.63, No.760, 2004, pp.109-120.

[16] Breitenbucher, R. et al., "Service life design for the Western Scheldt Tunnel," Durability of Building Materials and Components, No.8, 1999, pp.3-15.

[17] Val, D.V., Stewart M.G., "Life-cycle cost analysis of reinforced concrete structures in marine environments," Structural Safety, Vol.25, 2003, pp.343-362.

[18] Gonzalez, J. A., Andrade, C., Alonso, C., and Feliu, S., "Comparison of Rates of General Corrosion and Maximum Pitting Penetration on Concrete Embedded Steel Reinforcement," Cement and Concrete Research, Vol.25, No.2, 1995, pp.257-264.

[19] Costa, A., and Appleton, J., "Case studied of concrete deterioration in a marine environment in Portugal," Cement & Concrete Composites, Vol.24, 2002, pp.169-179.

[20] Michael, T.W., and Alberto, A.S., "Steel Corrosion in Submerged Concrete Structures — Part 1: Field Observations and Corrosion Distribution Modeling," Corrosion Science Section, 2016, pp.518-532.

[21] Gong, C.-Y. et al., "Long-term Field Corrosion Monitoring in Supporting Structures of China Xiamen Xiang'an Subsea Tunnel,"Acta Metallurgic Sinica,Vol.30,No.4, 2017, pp.399-408.

[22] He, Z., Liu, S., He, C., and Akiyama, M., "Structural damage process of an underwater shield tunnel in an aggressive environment," Proceedings of the Japan Concrete Institute, Vol.39, No.2, 2017, pp.1333-1338.